INTERNATIONAL
Standards Worldwide

Address 100 Barr Harbor Drive
PO Box C700
W. Conshohocken, PA
19428-2959 | USA

Phone 610.832.9500
Fax 610.832.9555
e-mail service@astm.org
Web www.astm.org

ERRATUM for **JAI104090**, **A Test Method for Monitoring Modulus Changes during Durability Tests on Building Joint Sealants**, by Christopher C. White, Donald L. Hunston, Kar Tean Tan, published in The Journal of ASTM International (JAI), Volume 9, Issue 2, February, 2012.

The correct Author listing should be: Christopher C. White, Donald L. Hunston, Kar Tean Tan, and Gregory T. Schueneman[4]

[4] USDA Forest Service, Forest Products Laboratory, One Gifford Pinchot Drive, Madison, WI 53726

Journal of ASTM International, Vol. 9, No. 2
Paper ID JAI104090
Available online at www.astm.org

Christopher C. White,[1] *Donald L. Hunston,*[2] *and Kar Tean Tan*[2]

A Test Method for Monitoring Modulus Changes during Durability Tests on Building Joint Sealants*

ABSTRACT: The durability of building joint sealants is generally assessed using a descriptive methodology involving visual inspection of exposed specimens for defects. It is widely known that this methodology has inherent limitations, including that the results are qualitative. A new test method is proposed that provides more fundamental and quantitative information about changes occurring in a sealant during durability testing. This test method utilizes a stress relaxation experiment to evaluate the non-linear viscoelastic behavior of sealants. In particular, changes in the time dependence of the apparent modulus can be observed and related to molecular changes in the sealant. Such changes often precede the formation of cracks and the ultimate failure of the sealant. This paper compares results obtained from the new test method and the currently used descriptive methodology.

KEYWORDS: sealant, durability, ASTM C719, ASTM C1519, stress relaxation, modulus

Introduction

Sealants are filled elastomers that are used commonly in structures in order to prevent moisture penetration through gaps, joints, and other openings. These structures span a wide range of diverse applications, including transportation vehicles and medical equipment. The greatest use of sealants, however, is in construction. Studies in the construction industry have indicated a 50% failure rate in less than 10 years and a 95% failure rate within 20 years after installation [1–3]. What makes these failures particularly detrimental is that sealants are often used in areas where moisture induced degradation is difficult to monitor and expensive to repair. Consequently, sealant failure is frequently detected only after considerable damage has occurred. In the housing market, premature failure of sealants and subsequent moisture intrusion damage significantly contribute to the $\$65 \times 10^9$ to $\$80 \times 10^9$ spent annually on home repair [4]. The environmental durability, therefore, is the most demanding requirement of a sealant, as it is the property that ultimately determines the long term service life.

Over the past few decades, extensive efforts have been devoted to investigating environmental effects on the long term durability of sealants and to investigating degradation mechanisms [5–8]. However, the accurate prediction of in-service performance in less time than required for field tests and tests on structures has remained an unsolved scientific issue. One of the main stumbling blocks to its solution is a lack of reliable methods for accurately quantifying the environmental degradation factors in the laboratory and field. Degradation measurements in the descriptive methodology usually involve visual evaluations of physical performance, including crack and chip size, chalking behavior, and color change. Although such a methodology can relate to a customer-perceived failure mode, it is qualitative and time consuming and provides little insight into the mechanisms leading to these macroscopic changes. This makes it difficult to develop models for accurately predicting sealant service life. An approach embedded in materials science could provide theoretical insight into the degradation mechanisms, help develop predictive models, and facilitate the establishment of a quantitative link between field and laboratory exposure results.

Manuscript received June 1, 2011; accepted for publication October 27, 2011; published online December 2011.

[1]Engineering Laboratory, Materials and Construction Research Division, National Institute of Standards and Technology, 100 Bureau Dr., Stop 8615, Gaithersburg, MD 20899-8615 (Corresponding author), e-mail: christopher.white@nist.gov

[2]Engineering Laboratory, Materials and Construction Research Division, National Institute of Standards and Technology, 100 Bureau Dr., Stop 8615, Gaithersburg, MD 20899-8615.

*Certain commercial products or equipment are described in this paper in order to specify adequately the experimental procedure. In no case does such identification imply recommendation or endorsement by the National Institute of Standards and Technology (NIST), nor does it imply that the item identified is necessarily the best available for the purpose.

The limitations of descriptive methodology have prompted the sealant community to seek improvements in the testing of sealant materials. A recent paper [9] presented a new method that was developed in cooperation with the sealant industry and which offers a solution to some of the issues inherent to the current approach. In this new method, a stress relaxation measurement was employed that monitors temporal changes in stress for a sealant subjected to a fixed strain. From this information, an apparent modulus versus time curve is generated. The magnitude and time dependence of this apparent modulus are related to the molecular structure of the sealant. By monitoring how this modulus changes with exposure time in a degradation experiment, one can estimate changes in the molecular structure of the sealant. Changes in the modulus over time also provide crucial information about how a sealant responds to the stresses imposed by the expansion and contraction of a structure over the diurnal cycle.

In a recent ASTM round robin for ASTM C1519-10, "Standard Test Method for Evaluating Durability of Building Construction Sealants by Laboratory Accelerated Weathering Procedures," four sealant samples were subjected to a series of laboratory accelerated weathering procedures and then evaluated using the usual visual inspection methods. The purpose of this paper is to evaluate specimens from this round robin using the new test method and to compare these results against results obtained from conventional evaluations.

Experiment

Materials

The ASTM round robin utilized four sealants that are typical of commercial materials: a silicone, modified polyester, an acrylic, and polyurethane. Specimens were provided to different laboratories. Each laboratory exposed the specimens according to the ASTM C1519-10 protocol and evaluated them after exposure via visual inspection. The specimens were fabricated by curing the sealant between two metal beams in the geometry shown in Fig. 1. This is similar to the geometry specified in ASTM C719 [10]. The specimens were fabricated by one of the primary manufacturers of sealants and were arbitrarily identified by the letters A through D. Specimens of each type of sealant were obtained from one of the participants in the round robin. For each sealant, five replicate specimens were provided: two fresh specimens having no exposure history, and three specimens after exposure according to the round robin protocol.

The specimen geometry used here is a widely accepted industry standard; however, unlike the simple dog-bone geometry, the sealant is constrained where it is attached to the metal bars. Consequently, when stretched, the center region of the sealant can contract laterally, but the sealant adjacent to the metal bars cannot. This means that deformation is not uniform throughout the sample, and an apparent modulus calculated from these tests, E_a, will be different from that obtained in a simple tension test with a dog-bone specimen, E. It is customary to treat this difference by defining a parameter, S, known as the shape factor, where $E_a = S \times E$. As the goal for the test procedure developed in this work is for comparisons using a single geometry, these results will be presented in terms of E_a.

Characterization

Details of the new test method are described elsewhere [9]; briefly, it involves two steps: a preconditioning step and the property measurement step. In the test, the two metal beams containing the sealant specimen are pulled in tension in the direction perpendicular to the long axis of the specimen. The strain history is schematically shown in Fig. 2. In the first step, the specimens were subjected to two loading-unloading-recovery

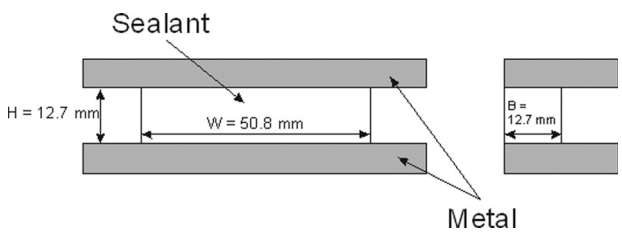

FIG. 1—*Schematic illustration of the test geometry used (left side is front view, right side is cross-section).*

cycles. The motivation for this step is to quantify the Mullins effect and eliminate its influence in the subsequent characterization measurement. In order to do this, the maximum strain in the two cycles must be larger than any strain seen in the specimen's previous history, and the same maximum strain must be used whenever the procedure is conducted, so results can be compared. For the experiments here, a maximum tensile strain of 26% was employed. This strain level was chosen because it exceeded the typical test movements of ±12.5% and ±25% used in ASTM C719. In addition, 26% strain should not be large enough to introduce any damage into the specimen. The loading-unloading tests utilized a crosshead speed of 2.64 mm/min so that the total time under load (t_o in Fig. 2) was 150 s. In order to allow for viscoelastic recovery, the specimen was held at 0% strain for 1500 s ($10t_o$) between cycles and before the next step. The test procedure developed in Ref 9 assumes that there is complete or nearly complete recovery in the time period. The criterion was that the compressive stress required in order to maintain zero strain at the end of recovery be less than 1.5% of the maximum stress achieved during the tensile cycles. To evaluate the Mullins effect [9], the loading curves on the two cycles were compared, and the magnitude of the effect was defined as the fractional drop in stress between the first and second loading curves at a particular strain level λ_x

$$\text{Magnitude of Mullins} = \frac{\sigma_1(\lambda_x) - \sigma_2(\lambda_x)}{\sigma_1(\lambda_x)} \tag{1}$$

where σ_1 and σ_2 represent the stresses during the first and second loadings. At very low strains, the magnitude of the Mullins effect is difficult to determine because the experimental uncertainty is very high. In this range, small differences in the position of zero strain generate large differences in the Mullins effect. In contrast, as the strain approaches the maximum value achieved during the loading cycle, the Mullins effect approaches zero. Between these extremes, however, there is a range of strains at which the magnitude of the Mullins effect remains relatively constant, changing by 10% or less. In the experiments here in which the maximum strain in the loading curves is 26%, the magnitude of the Mullins effect was determined at strains of 10%, 15%, and 20%.

Once the Mullins effect was quantified and eliminated, the viscoelastic properties of the sealant were measured in the second step of the procedure using a stress relaxation experiment (see Fig. 2). The specimens were loaded rapidly (70 mm/min) in tension to a maximum tensile strain of 18%, which was chosen arbitrarily between two limits, i.e., it must be significantly less than the strain level used in the Mullins cycles while not being so low that accurate measurements of strain and load become difficult. Once this strain level was attained, the specimen was held at that strain while the load was monitored as a function of time. The specimen reached the hold strain in just under 1 s. Data points during the first 5 s after loading commenced were ignored in order to eliminate confounding effects due to our inability to instantaneously load a specimen to the predetermined strain.

From the stress relaxation data, E_a was calculated using a relationship based on the statistical theory of rubberlike elasticity [9,11–13]

$$E_a(t, \lambda) = \frac{3L(t)}{WB(\lambda - \lambda^{-2})} \tag{2}$$

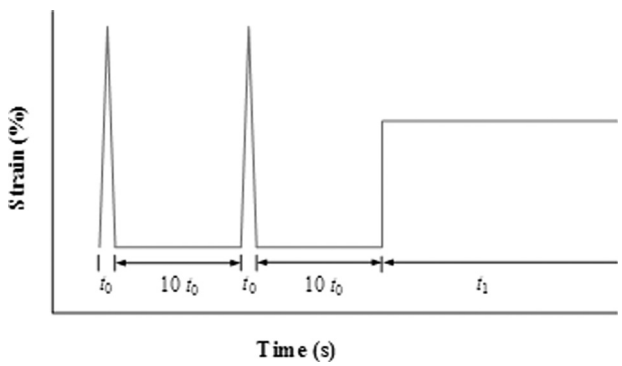

FIG. 2—*Strain history used for Mullins cycles and stress relaxation tests.*

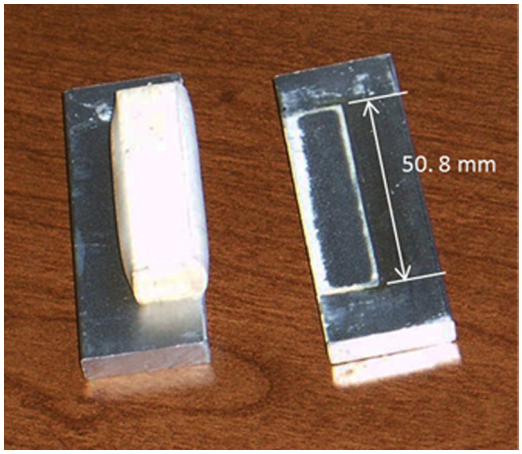

FIG. 3—*Illustration of debonded sealant B*.

where:

W and B = width and breadth of the sealant (Fig. 1),
L = load,
t = time, and
λ = extension ratio, which is given by

$$\lambda = 1 + \frac{\Delta}{H} \tag{3}$$

where:

Δ = crosshead displacement, and
H = undeformed height of the sealant.

Results and Discussion

The results from the visual observations made in the ASTM round robin after exposures are as follows: Sealant B exhibited complete adhesive failure during the test, with separation primarily between the sealant and the metal beam (Fig. 3). Moreover, these specimens' dimensions exhibited permanent deformation as seen in Fig. 3. Sealant A did not fail, but it also exhibited permanent deformation. In addition, Fig. 4 shows that the metal beams were no longer parallel, suggesting that specimen loading might not have been symmetric. Other than the permanent deformation, however, sealant A showed no signs of cracking, debonding, or color change. Sealants C and D displayed no visual changes over the stress relaxation period.

During the Mullins cycles, all four sealants met the criterion for complete or nearly complete recovery. This was true despite the observation above that suggests sealants A and B might exhibit permanent deformation if t_o is sufficiently large. Figure 5 shows the average magnitude of the Mullins effect for two samples of each sealant determined at a strain of 15%. Average values from tests on the exposed samples

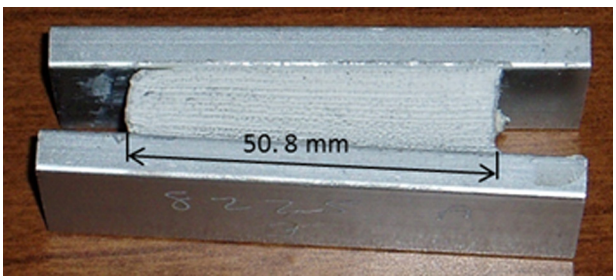

FIG. 4—*Illustration of distorted sealant A*.

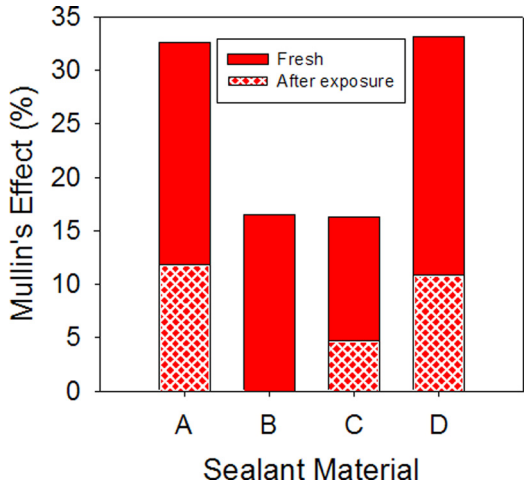

FIG. 5—*Average magnitude of the Mullins effect for the two samples of each sealant, determined at a strain of 15%.*

are shown as the cross-hatched area in each bar (no exposed data are available for sealant B specimens because they failed during the exposure tests). Similar results were obtained at strains of 10% and 20%. Note first that sealants A and D show a larger Mullins effect than sealants B and C. This indicates that the network structures in A and D have more junction points that can be disrupted by strains of 26% than do those in sealants B and C. Tests on specimens after exposure show a Mullins effect that is much less than that observed for fresh specimens but well above zero. Two hypotheses could explain this observation, either when considered on their own or in combination. First, if in the exposure tests the maximum strain never reached 26%, some Mullins effect would be expected in the characterization experiments. Second, a number of weeks passed between the exposure tests and the characterization experiments, and the specimens were under no load during this period. It has been shown [9] that many sealants recover (at least partially) some of the Magnitude of Mullins effect during such a period with no strain applied.

Figure 6 shows stress relaxation curves for all four fresh specimens. A wide variation in the stress relaxation modulus curves for the four sealants is apparent. Sealants A and D are virtually indistinguishable over the range of times tested. Relative to the range of modulus seen in previous sealant testing [9], sample B is near the soft end of the range, whereas sealant C is near the firm end. At very short times, sealants A and D display an upturn toward a glassy modulus, suggesting that they might have higher glass transition temperatures than sealants B and C. The curve for sealant C shows a slight downturn at long times, suggesting that flow-like behavior or a secondary relaxation mechanism might occur in these specimens over extended periods of time. Sealants A, C, and D show a clear rubbery plateau, whereas sealant B exhibits a continuous decrease in modulus through the rubbery zone. This decrease, combined with the

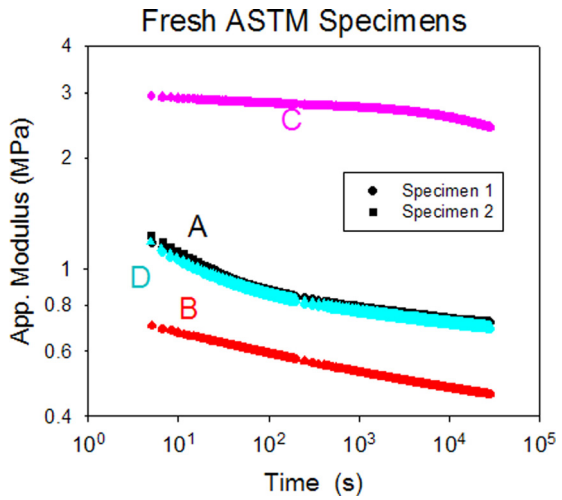

FIG. 6—*Stress relaxation curves of fresh specimens of sealants A, B, C, and D.*

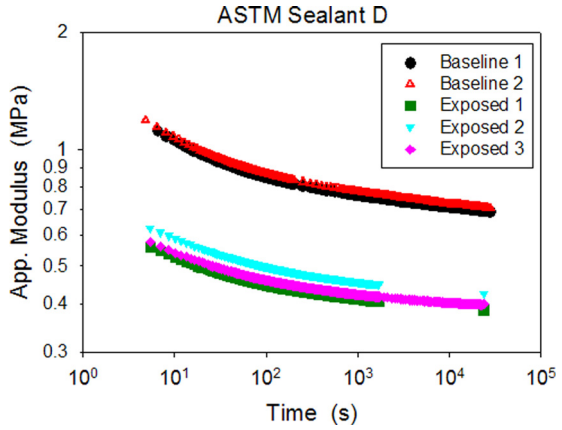

FIG. 7—*Stress relaxation curves of fresh and degraded specimens of sealant D.*

relatively low modulus in sealant B, suggests its network structure might have fewer junction points than the networks in the other sealants.

All three sealant B specimens failed during the stress relaxation period, so it was not possible to characterize the behavior of this sealant over the specified stress relaxation period. It is worth noting, however, that the lack of a plateau in the curve shown in Fig. 7 for this sealant is consistent with the generation of a permanent deformation in the specimen that is held under load for some time. It would be interesting to perform diffusion studies to see whether the relatively low density of junction points in the network might facilitate migration of environmental species, such as water, into the specimen, because this could weaken the interface between the sealant and metal.

As noted above, the visual examination of the exposed C and D specimens revealed no visible changes in the physical appearance of these sealants. The characterization curves, however, show that molecular changes have occurred in these sealants. The stress relaxation behaviors after exposure are dramatically different, as shown in Figs. 7 and 8. Also included in these plots are the data from the tests on fresh specimens for comparison. The relaxation curves for sealant D shift down to approximately half of the values of the unexposed counterparts, though the shape of the relaxation curve remains unchanged. This means that the time-dependence of the apparent modulus is unaltered by exposure, at least in the range examined here. Although the precise mechanism governing the decrease in apparent modulus remains ambiguous, the results support a view that structural changes after exposure are brought about by a reduction in the density of effective junction points in the network structure. Likewise, the magnitude of apparent modulus for sealant C decreases after exposure by about 30%. Although the shapes of the curves are similar, there is a less distinct downturn at long times than seen with the fresh sealants.

As stated above, exposure of sealant A produced no cracks, debonds, or color change, but some permanent deformation was present (Fig. 4). Two of the three exposed specimens were deformed to the point that further exposure was not possible. Results of experiments on the third specimen are shown in Fig. 9.

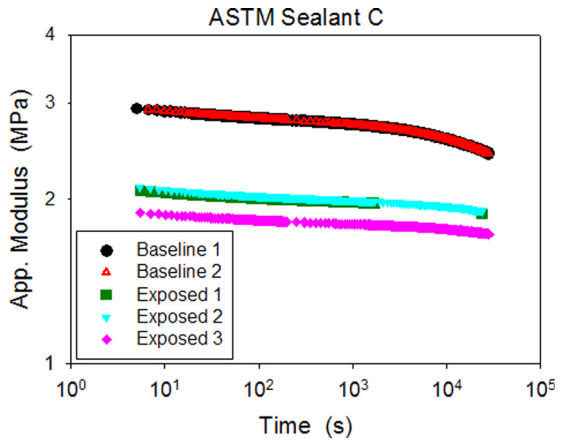

FIG. 8—*Stress relaxation curves of fresh and degraded specimens of sealant C.*

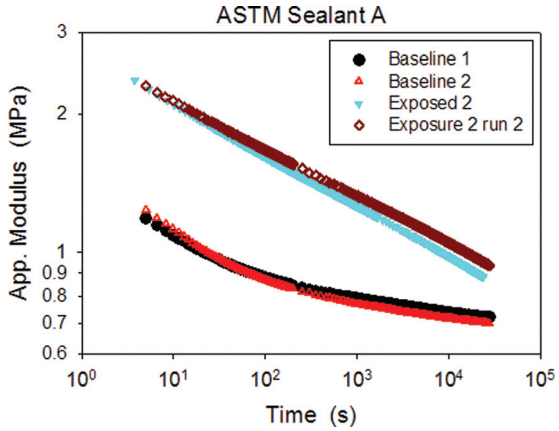

FIG. 9—*Stress relaxation curves of fresh and degraded specimens of sealant A.*

As with sealants C and D, the relaxation behavior for this specimen shows a dramatic change after exposure. Specifically, a noticeable increase in apparent modulus and substantial change in curve shape are clearly evident. The plateau region at long times is completely absent. This change in the time dependence of the apparent modulus indicates that drastic structural modification has occurred in the exposed specimens. To ensure the reproducibility of this result, the characterization was performed for a second time, and the relaxation curves for the two runs are virtually identical (Fig. 9).

In order to test this result, attempts were made to forcefully return the two highly deformed specimens of sealant A to their original dimensions. Wedges and clamps were inserted in order to achieve the original shape, and the specimens were held in this way for several weeks. After the wedges and clamps were removed, the samples were allowed to set for several days. Some of the deformation returned, but not enough to make the resumption of testing possible. Stress relaxation measurements were then performed on the specimens, and the results are shown in Fig. 10. The new data show trends similar to what was found with the initial exposed sample: the apparent moduli showed an increase, and the curve shape changed significantly. Although the differences between the new curves and the curve for the first exposed specimen could be the result of sample-to-sample variation, it is far more likely that the differences are artifacts introduced by testing deformed specimens. Consequently, although tests on deformed specimens might be useful for showing general trends, quantitative comparisons should be avoided.

The relaxation curves for fresh sealants A and D are identical (see Fig. 6). Moreover, neither shows any cracking, debonding, or color change after exposure. The stress relaxation tests, however, show that the effect of exposure on the two sealants is completely different. Whereas sealant D exhibits a decrease in modulus with no change in curve shape, sealant A shows an increase in modulus and a dramatic change

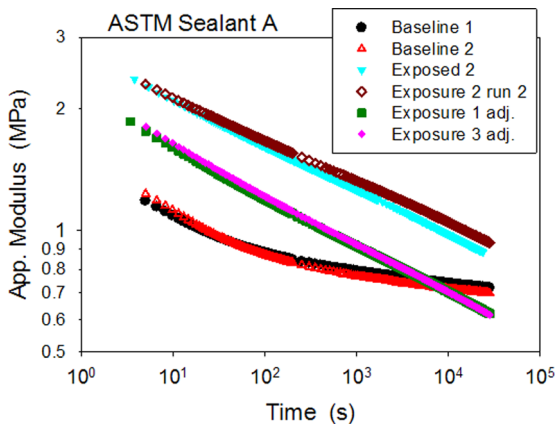

FIG. 10—*Different stress relaxation curves obtained from forcing distorted degraded specimens of sealant A to return to their original dimensions. The data for fresh specimens are also included for comparison.*

in curve shape (see Figs. 7 and 9). This result clearly demonstrates the different viscoelastic response of the sealants, which is not surprising given that their chemistries and formulations are different. This is potentially important information that could not be obtained from conventional visual inspection.

Conclusions

A test method for assessing the durability of building joint sealants using a stress relaxation approach has been examined. Specimens of four commercial sealant materials that underwent exposure conditions according to ASTM C1519-10 as part of a round robin were obtained and utilized as model systems in order to compare this new test method with the current, descriptive methodology involving visual inspection for defects. The results here show that the new test method not only allows meaningful quantitative evaluation of sealant characteristics but also provides qualitative information about the molecular structure of the sealants. It has been shown that important additional information that is not provided by visual inspection can be obtained by using this test method. This is particularly evident in the results for sealants C and D, for which visual inspection fails to reveal any changes after exposure even though significant changes are detected by the stress relaxation measurements. Consequently, the results here indicate that the viscoelastic characterization provides a robust methodology for quantitatively evaluating the durability of building joint sealants.

Acknowledgments

The support from a NIST/industry consortium on Service Life Prediction of Sealant Materials is greatly appreciated. Participating companies include DAP, Degussa, Dow Corning, Kaneka Texas, SIKA, Solvay, Tremco, and Wacker Silicones.

References

[1] Woolman, R., and Hutchinson, A., *Resealing of Buildings: A Guide to Good Practice*, Butterworth-Heinemann, Oxford, UK, 1994.
[2] Grunau, E., "Service Life of Sealants in Building Construction," *Research Report*, Federal Ministry for Regional Planning, Building and Urban Planning, Bonn, Germany, 1976 (in German).
[3] Chiba, R., Wakimoto, H., Kadono, F., Koji, H., Karimori, M., Hirano, E., Amaya, T., Sasatani, D., and Hosokawa, K., *Improvement System of Waterproofing by Sealants in Japan*, Japan Sealant Industry Association, Tokyo, Japan, 1992, pp. 175–199.
[4] "Expenditures for Residential Improvements and Repairs—1st Quarter," *Current Construction Reports*, U.S. Census Bureau, Department of Commerce, Washington, D.C., 2002.
[5] *Durability of Building and Construction Sealants and Adhesives, STP 1453*, A. T. Wolf, Ed., ASTM International, West Conshohocken, PA, 2004, pp. 385–398.
[6] White, C. C., Tan, K. T., Hunston, D. L., and Williams, R. S., *Service Life Prediction of Polymeric Materials: Global Perspective*, J. W. Martin, R. A. Ryntz, J. Chin, and R. Dickie, Eds., Springer, New York, 2008, pp. 115–128.
[7] Searle, N. D., and *Handbook of Sealant Technology*, K. L. Mittal and A. Pizzi, Eds., CRC Press, Boca Raton, FL, 2009, pp. 93–142.
[8] Wolf, A. T., *Handbook of Sealant Technology*, K. L. Mittal and A. Pizzi, Eds., CRC Press, Boca Raton, FL, 2009, pp. 143–189.
[9] White, C. C., and Hunston, D. L., "Characterizing the Non-Linear Viscoelastic Properties of Sealant Including the Mullins Effect," *Polym. Eng. Sci.*, Vol. 48(12), 2008, pp. 2317–2328.
[10] ASTM C719-93, 2010, "Standard Test Method for Adhesion and Cohesion of Elastomeric Joint Sealants Under Cyclic Movement (Hockman Cycle)."
[11] Taylor, C. R., Greco, R., Kramer, O., and Ferry, J. D., "Nonlinear Stress Relaxation of Polyisobutylene in Simple Extension," *J. Rheol.*, Vol. 20, 1976, pp. 141–152.
[12] Ferry, J. D., *Viscoelastic Properties of Polymers*, 3rd ed., John Wiley & Sons, Inc., New York, 1980.
[13] Ketcham, S. A., Niemiec, J. M., and McKenna, G. B., "Extension and Compression of Elastomeric Butt Joint Seals," *J. Eng. Mech.*, Vol. 122, 1996, pp. 669–677.

INTERNATIONAL
Standards Worldwide

Address 100 Barr Harbor Drive
PO Box C700
W. Conshohocken, PA
19428-2959 | USA

Phone 610.832.9500
Fax 610.832.9555
e-mail service@astm.org
Web www.astm.org

ERRATUM for **JAI104090**, **A Test Method for Monitoring Modulus Changes during Durability Tests on Building Joint Sealants**, by Christopher C. White, Donald L. Hunston, Kar Tean Tan, published in The Journal of ASTM International (JAI), Volume 9, Issue 2, February, 2012.

The correct Author listing should be: Christopher C. White, Donald L. Hunston, Kar Tean Tan, and Gregory T. Schueneman[4]

[4] USDA Forest Service, Forest Products Laboratory, One Gifford Pinchot Drive, Madison, WI 53726